

Effective Factors on the Generated Transient Voltage in the Wind Farm due to Lightning

M. A. Abd-Allah, Mahmoud N. Ali, A. Said*

Faculty of Engineering at Shoubra, Benha University, Egypt

*Corresponding author, e-mail: abdelrahman.ghoniem@feng.bu.edu.eg

Abstract

According to reports that had been published in many papers, wind turbines (WTs) fault due to lightning is one of the most difficult challenges. Lightning overvoltage lead to malfunction in the wind farm equipments. These improper functioning contain of malfunction electronic equipments and deformation of transformer winding and Surge arrester failures. The travelling waves which are generated due to high ground potential rise under lightning struck turbine cause these problems. To evaluate these cases, it must be performed an accurate analysis on the wave shape and level of the Lightning overvoltage and ground potential rise. This paper investigates the effective factors on the wave shape and level of the overvoltage, GPR and surge arrester burnout. These factors are included impulse Current-second characteristics, position of lightning, inception angle, multiple lightning strokes and chopped current. ATP-EMTP simulation program is applied to analyze the lightning over-voltage of onshore wind farm. This paper provides a practical procedure of lightning protection.

Keywords: WT's, current-second characteristics, lightning overvoltage, GPR, ATP/EMTP

Copyright © 2015 Institute of Advanced Engineering and Science. All rights reserved.

1. Introduction

With a rapid growth in wind power generation, lightning hazard to wind turbines (WTs) has come to be regarded with more attention. Due to their great height, distinctive shape, and exposed location, WT's are extremely vulnerable to lightning stroke. After a WT is struck by lightning, high lightning current flows through the WT and causes considerable damage to electrical equipment inside the WT structure and wind turbine nacelle results stop of the generator operation and probably expensive repairs [1].

In order to decrease downtime, repairs and blade damaged. Protecting the blade is very important and well-designed lightning protection is a necessity for this equipment so Modern wind turbine blades are made of insulating materials such as glass fiber reinforced plastic (GFRP) as a common material or wood epoxy. The lightning protection of wind turbine blades can be classified as receptor, metallic cap, mesh wire, and metallic conductor as reported in IEC-61400-24 standards.

In general, the problem of lightning protection of wind turbine blades is to conduct the lightning current safely from the attachment point on the blade to the hub and then to the ground.

However another serious problem known as "back-flow surge" which not only causes damages to the wind turbine that has been struck but also the other turbines that have not. The back-flow surge phenomenon has been defined as the surge flowing from a customer's structure such as a communication tower into the distribution line. High resistivity soil often makes Surge Arresters (SAs) at tower grounding systems operate in reverse and allow backflow of surge current to the grid. The phenomenon of surge invasion from a wind turbine that is struck by lightning to the distribution line in a wind farm is quite similar to the case of "back-flow surge" [2].

Due to significant influence on the wind farm behavior under lightning, the transient response must be either accurately analyzed. So in this paper wind farm component model is implemented using ATP_EMTP. Characteristics and hazards of back-flow surge in onshore wind farm are analyzed and discussed. Effective Factors on the Transient Voltage Generated in the Wind Farm due to Lightning are analyzed. These factors are included impulse Current-

second characteristics, position of lightning, inception angle, multiple lightning strokes and chopped current. This paper provides a practical procedure of lightning protection.

2. Description and Modeling of the Onshore Wind Farm

Figure 1 shows layout of onshore wind farm composed of two identical wind power generators. Boost transformers for the generators are installed in vicinity of the wind turbine towers. All boost transformers are connected to the grid via grid-interactive transformer by overhead distribution line. Surge arresters are inserted to the primary and secondary sides of the boost and grid-interactive transformers.

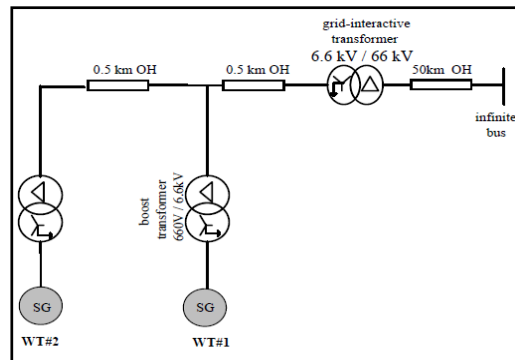


Figure 1. Wind farm model [2]

Table 1 gives the required data for modeling the generators of the wind turbines, transmission line and transformers.

Table 1. Wind Turbines, Transformers Data and connected line data [2]

Wind Turbine Model(Synchronous Generator- Y connected)	
Voltage (line rms)	0.660 [kV]
Rated power	1.0 [MVA]
Leakage reactance	0.1 [H]
Frequency	60.0 [Hz]
Transformer Model (Boost, Grid-Interactive)	
Connection method	Y / Δ , Y / Δ
Voltage (line rms)	0.660/6.6 [kV], 66.0/6.6 [kV]
Rated power	1.0 [MVA], 10.0 [MVA]
Leakage reactance	0.15 [p.u]
Copper losses	0.005 [p.u]
No-load losses	neglected
Line Model (values at 60 Hz)	
positive / zero phase resistance [Ω/Km]	0.00105/0.021
Positive / zero phase inductance [mH/Km]	0.83556/2.50067
Positive / zero phase capacitance [nF/Km]	12.9445/6.4723

A current function model called Heidler is now used widely to model a lightning current [3-5]. Equation (1) represents the lightning current. A 400 Ω lightning path resistance was connected shunt to the simulated natural lightning as shown in Figure 2.

$$i(t) = I_o \frac{(t / \tau_1)^2}{[(t / \tau_1)^2 + 1]} e^{-t / \tau_2} \tag{1}$$

Where I_o : the peak of current, τ_1, τ_2 : time constants of current rising and dropping.

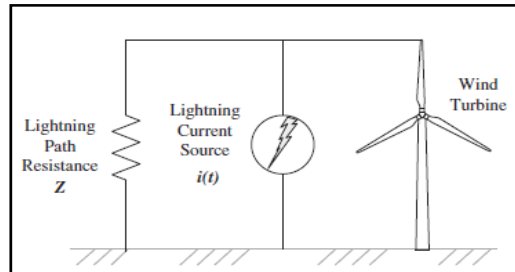


Figure 2. Lightning current model

The down conductor in the blade and the wind turbine tower have been considered as a lossless transmission line and they were estimated according to following experimental equation [4-7], Equation (2), where the down conductor and the tower often were treated as a cylindrical conductor.

$$Z = 60 (\ln \frac{2\sqrt{2}}{r} h - 2) \tag{2}$$

Where, Z is the surge impedance, r and h are the radius and height of the cylinder, respectively. The wind tower is taken as an iron vertical conductor of 60 m height and 3.0 m radius.

The overhead lines are considered and represented by single-phase positive wave impedance (i.e. Surge impedance) with the light velocity.

$$Z_0 = \sqrt{L / C} \ \Omega \tag{3}$$

$$v = \frac{1}{\sqrt{LC}} \quad m / s \tag{4}$$

Where, C and L are the capacitance and inductance of line, respectively, Z_0 is the surge impedance and v is the propagation velocity [3, 8].

A simplified model of surge arrester was derived from IEEE model [9, 10]. The model circuit is shown in Figure 3. This model is composed by two sections of nonlinear resistances usually designated by A_0 and A_1 which are separated by inductance L_1 and L_0 . A parallel resistance R_p (about 1 M Ω) is added to avoid the numerical instability of the combination of the current source and nonlinear elements.

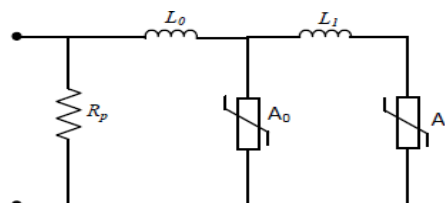


Figure 3. Pinceti and Giannettoni model

In case medium and high voltage levels the inductances L1 and L0 in the model are in μH and calculated using:

$$L1 = \frac{1}{4} \frac{Ur1/T2 - Ur8/20}{Ur8/20} Un \quad (5)$$

$$L0 = \frac{1}{12} \frac{Ur1/T2 - Ur8/20}{Ur8/20} Un \quad (6)$$

In case low voltage levels the inductances L1 and L0 in the model are in μH and calculated using:

$$L1=0.03Un \quad (7)$$

$$L0=0.01Un \quad (8)$$

Where Un is the arrester rated voltage in kV, $Ur1/T2$ is the residual voltage at 10 kA fast front current surge ($1/T2 \mu\text{s}$). $Ur8/20$ is the residual voltage at 10 kA current surge with $8/20 \mu\text{s}$ time parameters.

The nonlinear characteristics of the two elements A0 and A1 are based on the pu data published in [11]. In this paper Ground system model is based on the nonlinear performance of the grounding resistance with high currents i.e. high voltage, high frequency model [13]. The nonlinearity nature of the ground resistance can be represented by a nonlinear resistance, R_t , whose value is given as [12];

$$\begin{cases} R_t = R_0 \rightarrow \text{For } (i < I_g) \\ R_t = \frac{R_0}{\sqrt{1 + \frac{i}{I_g}}} \rightarrow \text{For } (i \geq I_g) \end{cases} \quad (9)$$

Where, i is the current through the rod (kA), and I_g is the critical current for soil ionization (kA) which is given by:

$$I_g = \frac{E_0 * \rho}{2\pi R_0^2} \quad (10)$$

Where, E_0 is the critical soil ionization gradient and R_0 constant resistance and given by:

$$R_0 = \frac{\rho}{2\pi l} \left\{ \ln \frac{4l}{a} - 1 \right\} \quad (11)$$

Where, ρ is the soil resistivity ($\Omega\cdot\text{m}$), L is the electrode length (m) and a is the electrode radius (m).

3. Results and Discussion

In this study, the lightning stroke is taken as striking wind turbine (WT#1) as shown in Figure 4. Lightning current waveform of $51\text{kA}-2/631\mu\text{s}$ is used in this study.

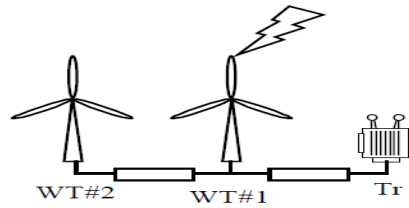
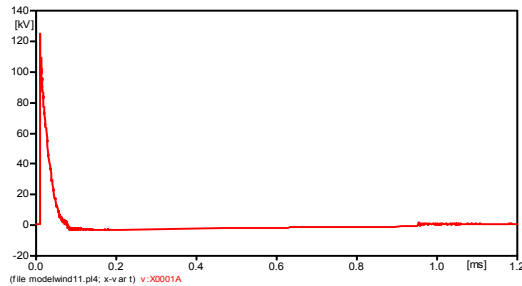


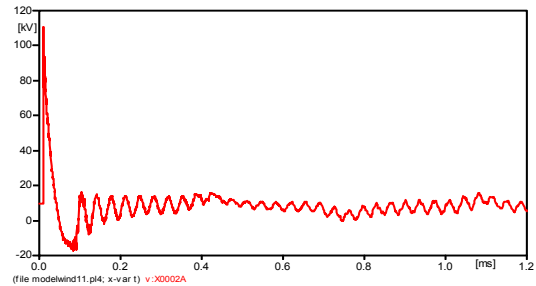
Figure 4. lightning hit WT#1 [3]

In this case, voltages at four different locations (at Generator terminal with lightning hit, 6.6 kV sides of the boost transformers and the grid-interactive transformer) are taken for analysis.

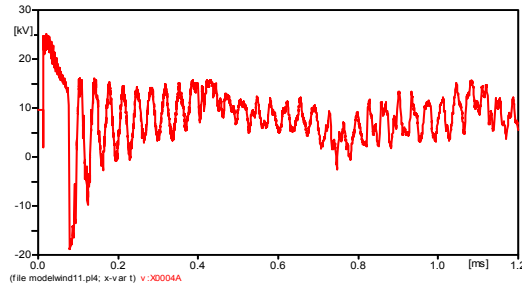
Figure 5 shows the voltage waveforms and its peak value at different locations of the wind farm. It is observed that the peak magnitude of the generated overvoltage at WT#1 generator terminal can be as high as 125kV, at (WT#1) boost transformer secondary side reach to 111kV, at (WT#2) boost transformer secondary side reach to 25kV and at grid reach to 27kV. Also these wave forms oscillate with high frequency. It is clear that the surge hitting WT#1, which was struck by lightning, was propagated to the adjacent turbine and the grid through collecting point.



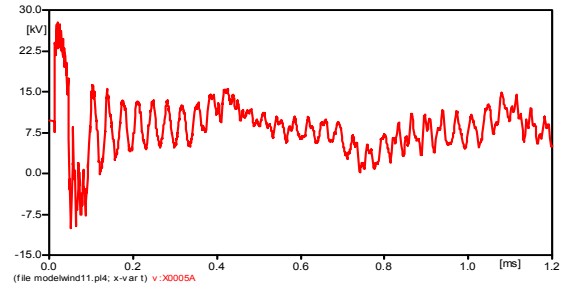
(a) Voltage on Generator WT#1



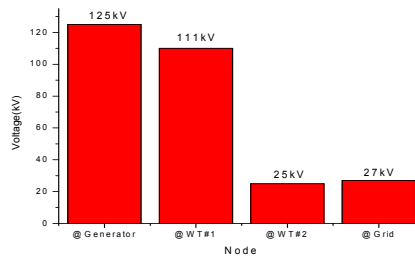
(b) Voltage at boost transformer voltage (WT#1)



(c) Voltage at boost transformer voltage (WT#2)



(d) Voltage at primary grid voltage



(e) Peak value of voltage at different location in wind farm

Figure 5. Voltage waveforms through phase (a)

Figure 6 shows the GPR wave form at WT#1 and its peak value at different locations of the wind farm. It is observed that the peak magnitude of the GPR at WT#1 reach to 126kV , at (WT#2) reach to 8kV and at grid reach to 10kV. It is clear that the GPR is enough high to cause Back flow current.

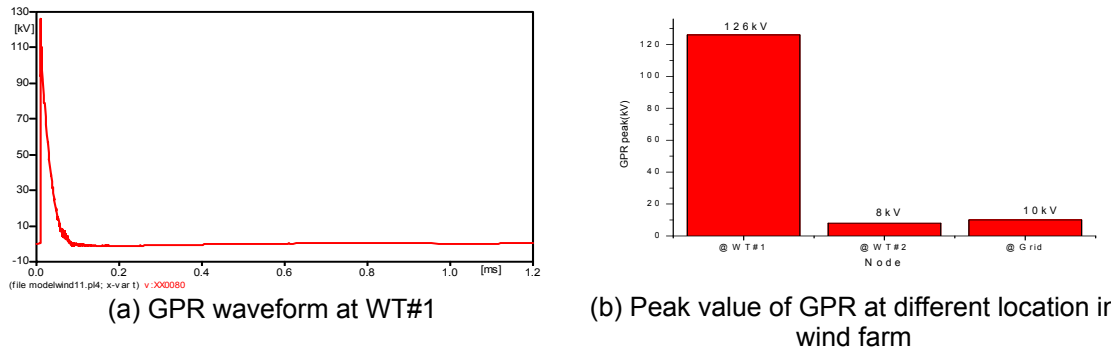


Figure 6. GPR at different locations of the wind farm

The Surge Arrester (SA) burnout depends on the heat produced by the current flowing through the arrester exceeds its thermal limit. The absorbed energy can be obtained in watt-hour [14]:

$$w = \int_0^T P(t) dt / 3600 \tag{12}$$

Where, P(t) is the instantaneous power in watt. The absorbed energy in kJ is calculated as:

$$\text{Energy} = 3,6 \times W \tag{13}$$

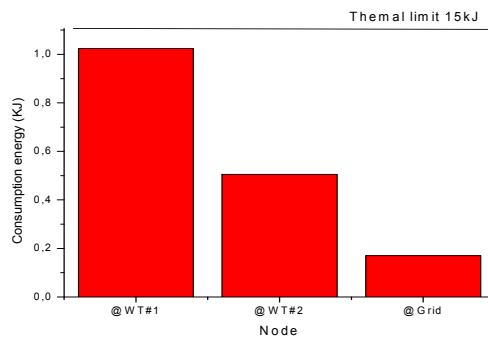
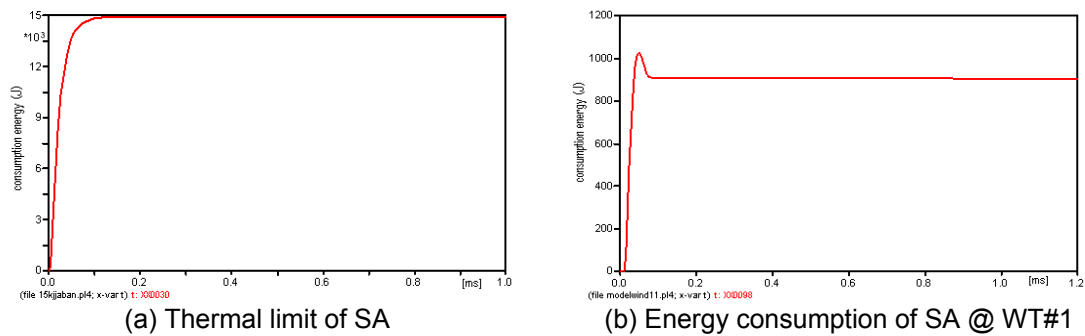


Figure 7. Energy consumption of surge arrester at different locations of the wind farm

Figure 7 shows the energy consumption of surge arrester through phase (a) located at 6.6 kV side of boost transformers at WTs#1, 2 and at the primary side of grid. It is observed that the SA in phase a at the wind turbine that was actually struck consumed the largest energy, then SA at WT#2 and Grid consume less energy. The result shows that the absorbed energy of surge arresters at turbines and grid are higher but within limits.

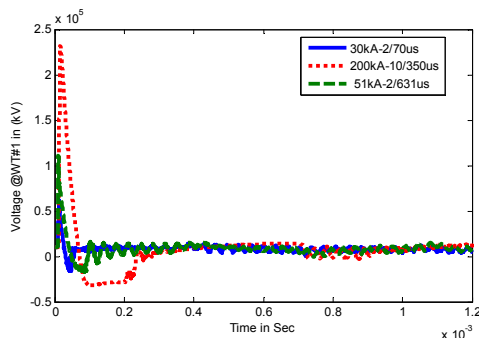
4. Effective Factor on Generated Transient Voltages.

4.1. Effect of Lightning Type

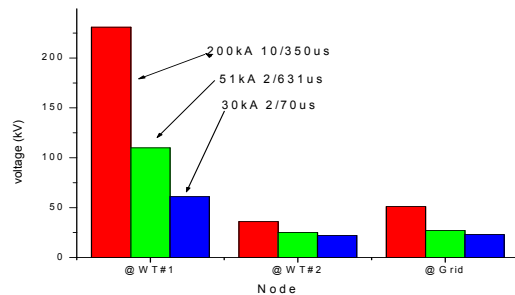
Three lightning surges are used in this investigation [15, 16]. Table 2 gives the characteristics of each lightning surge.

Table 2. Lightning Surges Characteristics (Standard for Lightning Protection and Lightning Strength in Japan)

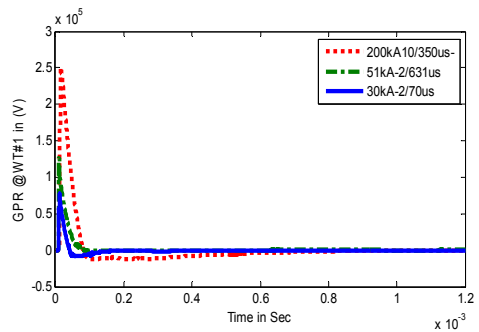
Lightning type	Peak value [kA]	Front time [μ s]	Tail time [μ s]
Japan	Summer #1	30.0	2.0
	Winter #2	51.0	2.0
Case #3	200.0	10.0	350.0



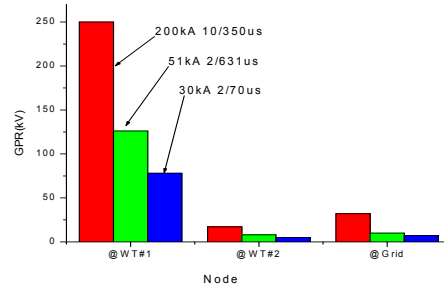
(a) Voltage waveforms @WT#1



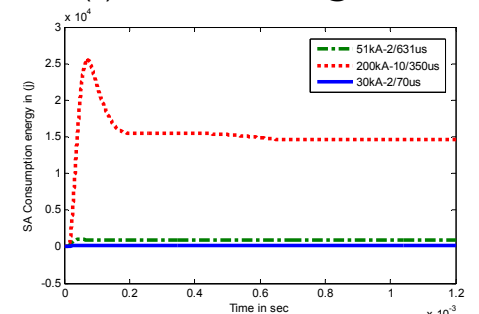
(b) Comparison between peak values of voltage at each node



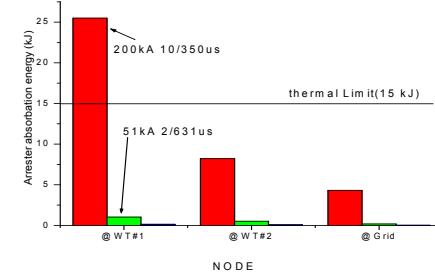
(c) GPR waveforms @WT#1



(d) GPR at different locations of the wind farm



(e) SA consumption energy waveforms @WT#1



(f) comparison of SA energy consumption at different location

Figure 8. overvoltages, GPR and arrester absorption energy at different locations of the wind farm under different type of lightning

Figure 8 shows the overvoltage, GPR and consumption energy of arrester through phase a located at 6.6 kV side of boost transformers at WTs#1, 2 and at the primary side of grid comparison with varying the lightning peak value. It is observed that the peak value of the overvoltage and GPR at WT#1 reach to 231kV and 250kV respectively, also the energy consumption of the SA surpassed their thermal limitation only at the WT#1 under lightning surge #3. This is due to high peak value of lightning surge #3. It is clear that the lightning surge strikes the wind tower is more significant under high crest lightning surge #3.

4.2. Effect of Lightning Parameter Front Time

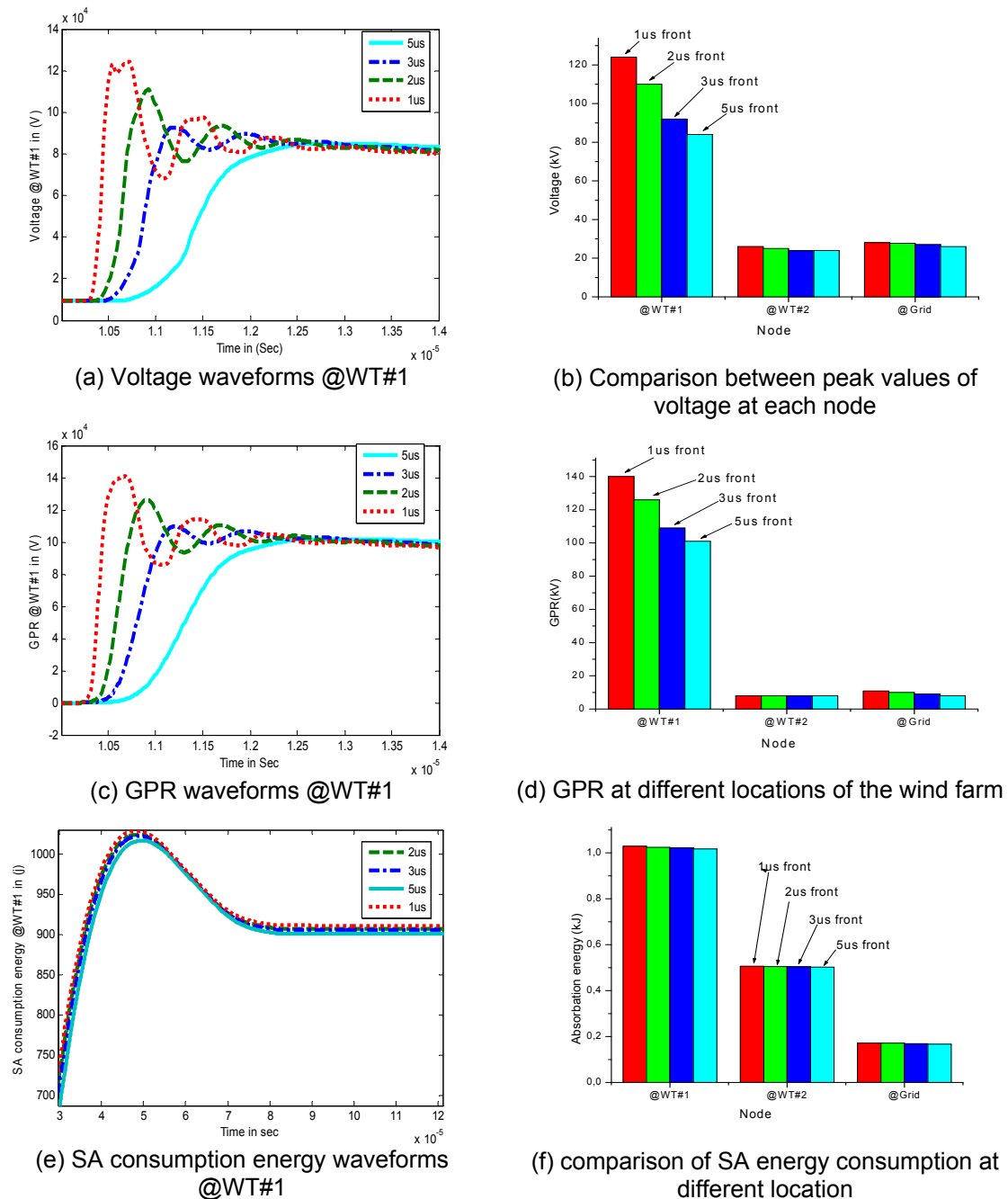
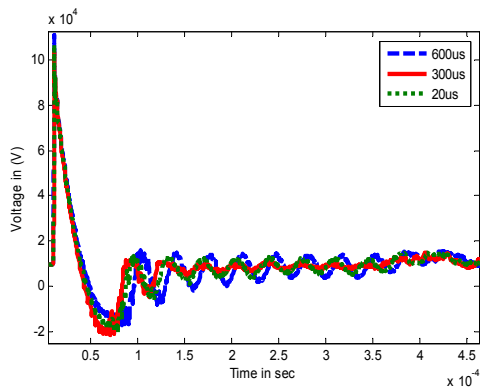


Figure 9. Overvoltages, GPR and arrester absorption energy at different locations of the wind farm under different lightning front time

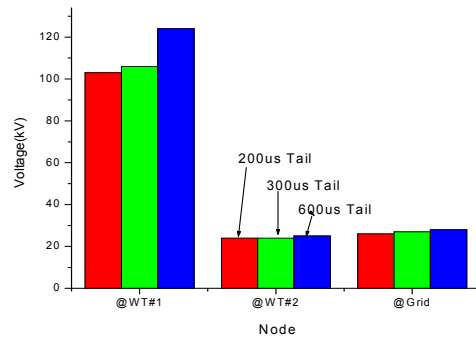
The lightning strokes with different front time ($1\mu\text{s}:5\mu\text{s}$) [17] are studied to show the effect of them. Figure 9 shows the comparison of voltage, GPR and arrester absorbing energy with varying lightning front time. The results indicate that the maximum voltage and the GPR located at turbines and grid are decreased with increasing front time of lightning. Also, the absorbed energy by the arresters located at the non-thunderstruck turbines and grid decrease with increasing front time of lightning.

This indicates that for the same current magnitude, the fast rising current dissipates to ground more quickly than the slow rising current. The faster fronted current pulse results in larger potential at feed point in the first moments because larger currents are forced to disperse into the ground through small parts of the electrode.

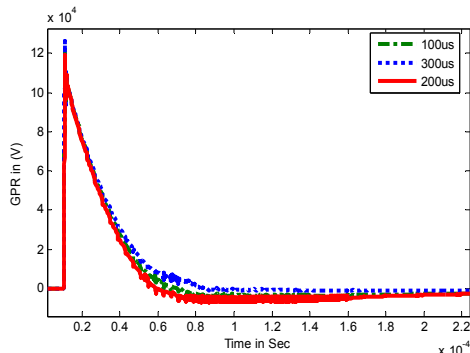
4.3. Effect of Lightning Parameter Tail Time



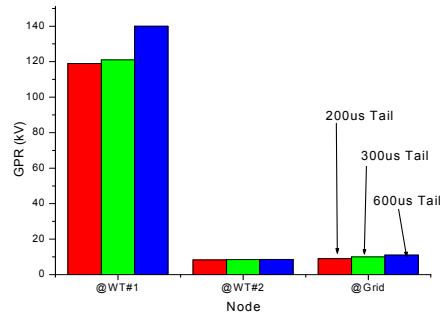
(a) Voltage waveforms @WT#1



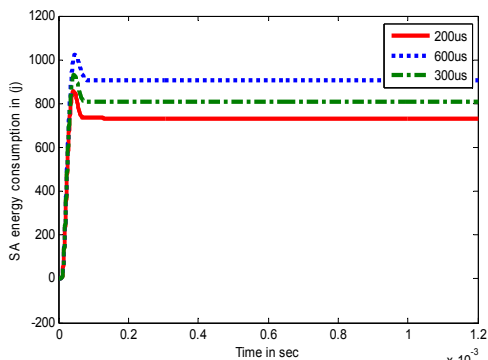
(b) Comparison between peak values of voltage at each node



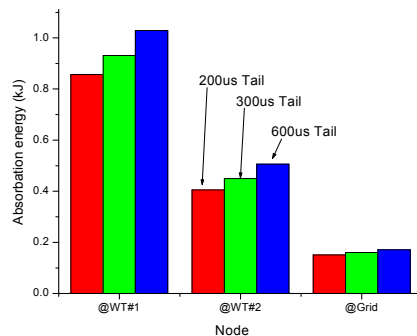
(c) GPR waveforms @WT#1



(d) GPR at different locations of the wind farm



(e) SA consumption energy waveforms @WT#1



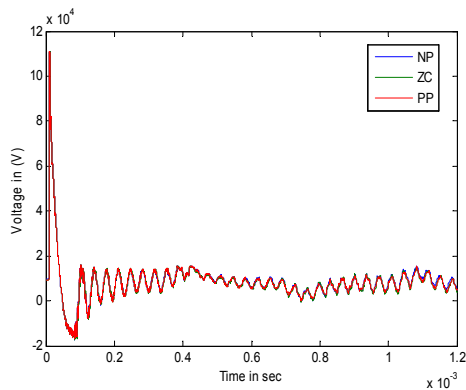
(f) comparison of SA energy consumption at different location

Figure 10. Overvoltages, GPR and arrester absorption energy at different locations of the wind farm under different lightning tail time

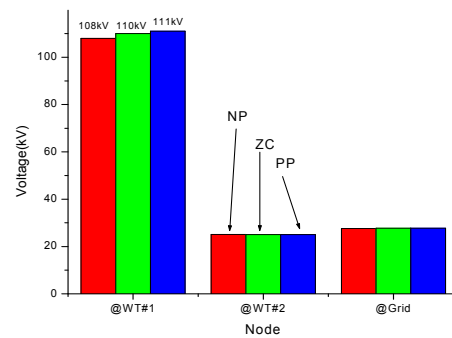
The lightning strokes with different tail time (200 μ s:600 μ s) are studied to show the effect of them. Figure 10 shows the comparison of voltage, GPR and arrester absorbing energy with varying lightning front time. The results indicate that the maximum voltage and the GPR located at turbines and grid are increased with increasing tail time of lightning. Also, the absorbed energy by the arresters located at the non-thunderstruck turbines and grid increase with increasing tail time of lightning.

This indicates that for the same current magnitude, the slow decay current dissipates to ground more quickly than the fast decay current. The slower decayed current pulse results in larger potential at feed point in the first moments because larger currents are forced to disperse into the ground through small parts of the electrode.

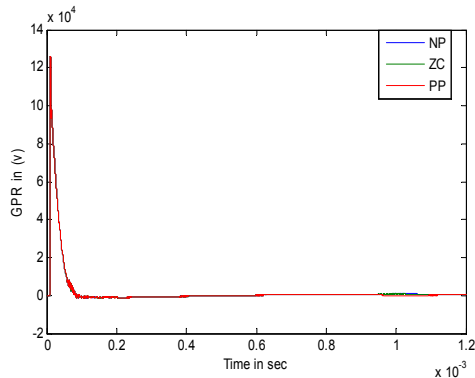
4.4. Effect of Lightning Inception Angle



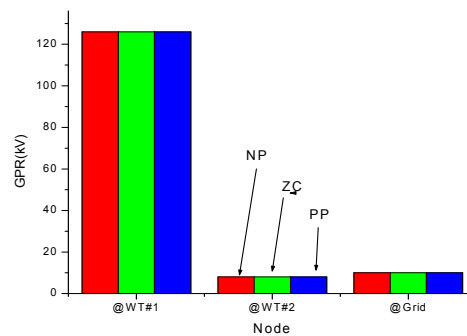
(a) Voltage waveforms @WT#1



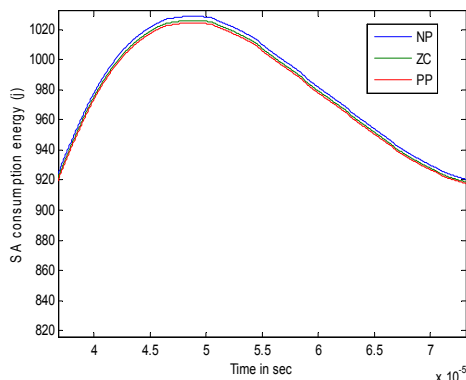
(b) Comparison between peak values of voltage at each node



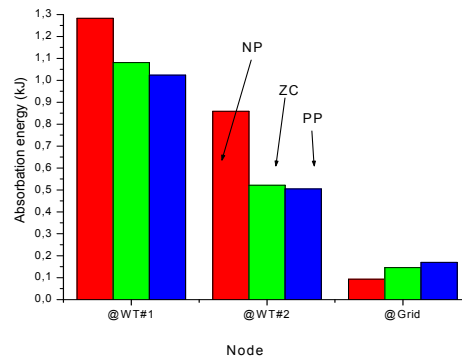
(c) GPR waveforms @WT#1



(d) GPR at different locations of the wind farm



(d) SA consumption energy waveforms @WT#1



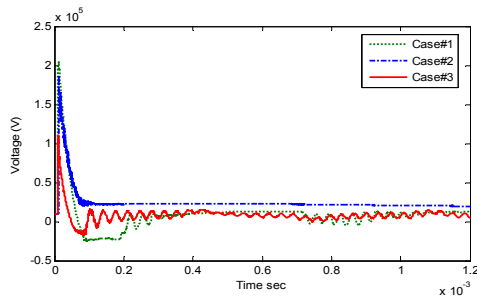
(e) comparison of SA consumption energy at different location

Figure 11. Overvoltages, GPR and arrester absorption energy at different locations of the wind farm under different lightning inception angle

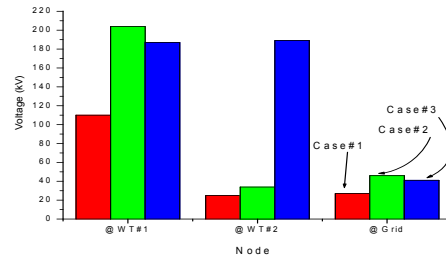
The impact of the inception angle is studied only with respect to phase a of voltage waveform, this is because of the phase differences between the three phases. Three different scenarios of lightning inception angle are studied. The first one is when the lightning hits the wind turbine WT#1 at the negative peak (NP) of voltage waveform of phase a. The second case is when the lightning hits it at the zero crossing (ZC). The third case is when the lightning hits at the positive peak (PP). Figure 11 shows the overvoltage, GPR and consumption energy of arrester through phase a located at 6.6 kV side of boost transformers at WTs#1, 2 and at the primary side of grid with varying the inception instant.

Figure 11 shows the absorbed energy of phase a surge arrester located at the 6.6kV side of boost transformers. The result shows that the absorbed energy of surge arresters at negative peak inception instant is within limits but higher than those at zero crossing and positive peak instants. This can be related to the fact that the lightning surge current in case of negative peak is higher than that of the case of zero crossing and positive peak. The reason is because the potential difference at the case of negative peak is higher than that in case of positive peak and zero crossing. But the consumption energy of SA at the grid is negative according to result at turbines. Also The GPR is independent of the inception instant on the wave. Also the surge propagation magnitude is quite dependent on the inception instant when the lightning hits the wind turbine.

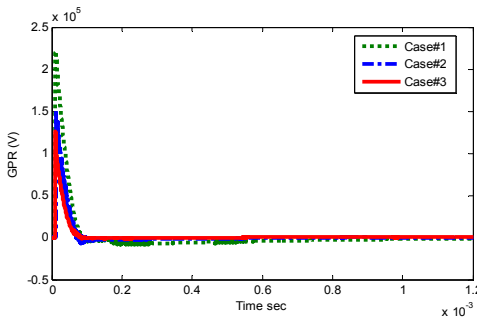
4.5. Effect of Different Lightning Location



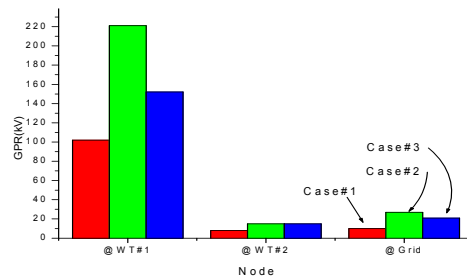
(a) Voltage wave form @WT#1



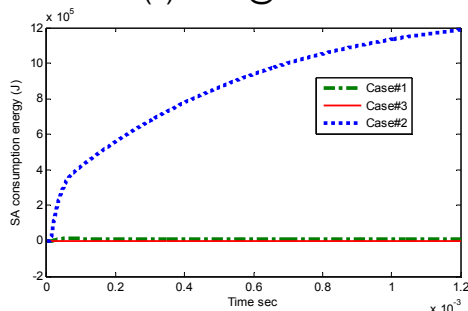
(b) Comparison between peak values of overvoltage at each node



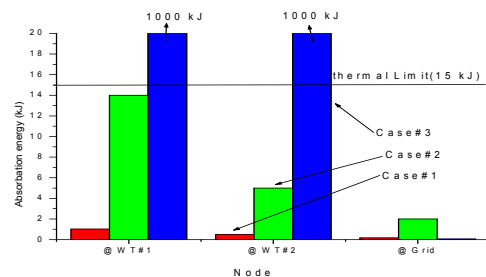
(c) GPR @WT#1



(d) GPR at different locations of the wind farm



(e) SA consumption energy of SA @WT#1



(f) comparison of SA energy consumption at different location

Figure 12. Overvoltages, GPR and arrester absorption energy at different locations of the wind farm under different lightning location

A different lightning strokes location is studied to show the effect of them. This investigation is under three different cases. The first case is direct Stroke occurs when lightning strike the boost transformer behind the wind turbine (Case#1). The second case is direct Stroke occurs when lightning stroke hit the distance TL between the turbines (Case#2). The last case is Backflow Current –Overvoltage when the lightning hits any part of wind turbine so lightning reach the ground resistance via down conductor (Case#3). Figure 12 shows the comparison of voltage, GPR and arrester absorbing energy at different turbine and grid with varying lightning position. The results indicate that the maximum voltage and the GPR located at struck turbine and grid are increased in case#1. Also, the absorbed energy by the arresters located at the non-thunderstruck turbines and thunderstruck increase and exceed thermal limit in case Case#2.

4.6. Effect of Multiple Lightning Strokes

Three selected of multiple lightning strokes, shown in Figure 13, with amplitudes of 18.6kA, 15kA and 12kA for the 1st, 2nd and 3rd strokes, with 1ms intervals were used [18]. Figure 14 gives the waveform of the single lightning stroke. Figure 15 to 19 shows waveform of overvoltage at WT#1 and energy consumption of arrester at WT#1 also shows the voltage, GPR and arrester absorbing energy at different turbine and grid under single and multi strikes. The results show that multiple strikes don't affect on peak value of overvoltage and GPR, but has a great effect on energy consumption of SA. From the results obtained; multiple lightning strokes which occur in real situations are much more severe than a single lightning stroke.

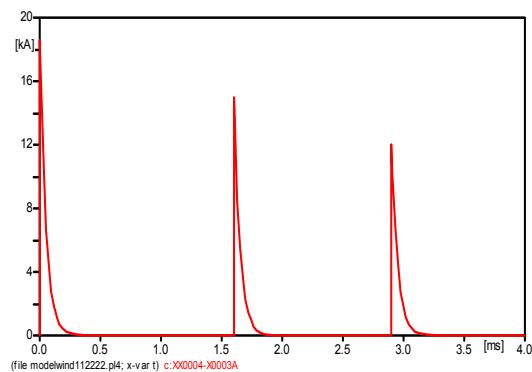


Figure 13. Waveforms of the 1st, 2nd and 3rd positive lightning strokes

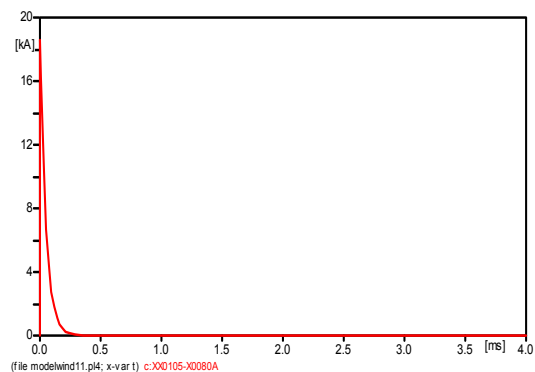


Figure 14. Waveform of the 1st injected lightning stroke

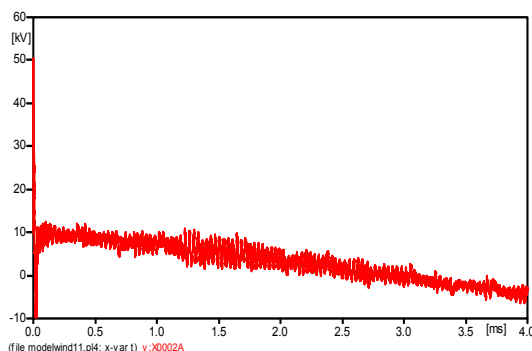


Figure 15. Voltage Waveform at WT#1 under single strike

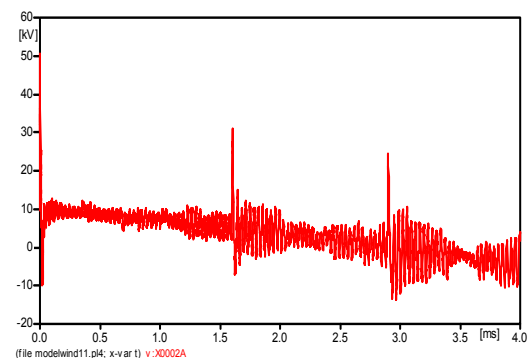


Figure 16. Voltage Waveform at WT#1 under multiple strike

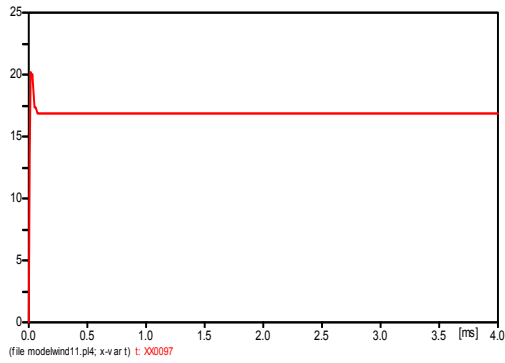


Figure 17. Consumption energy of arrester at WT#1 under single strike

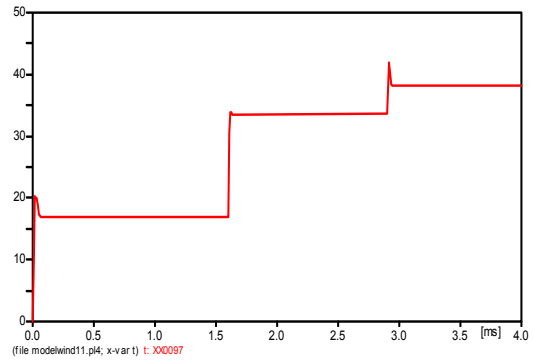
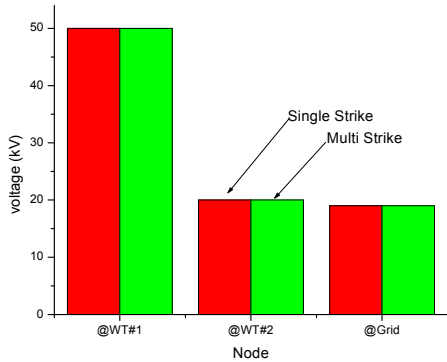
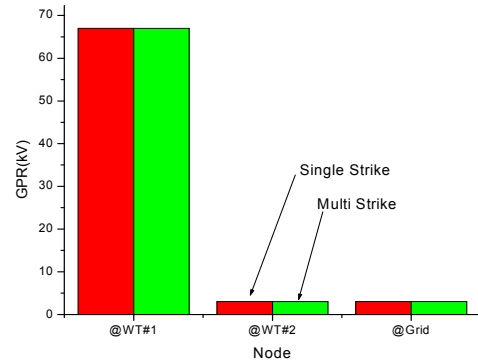


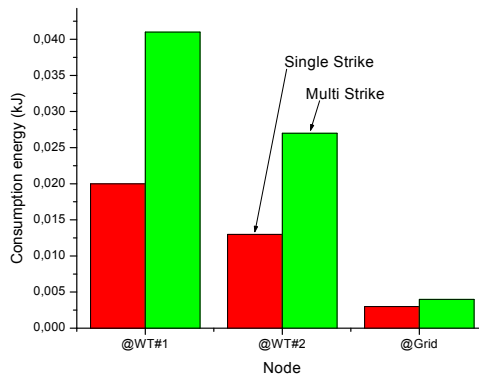
Figure 18. Consumption energy of arrester at WT#1 under multiple strikes



(a) peak values of voltage at each node



(b) GPR at different locations of the wind farm



(c) SA energy consumption at different location

Figure 19. Overvoltages, GPR and arrester absorption energy at different locations of the wind farm under different lightning

4.7. Effect of Chopped Current

Lightning strokes chopped at tail wave 0.1, 0.3, 0.5ms waveform are used. Figure 20 gives the waveform of the lightning chopped tail time simulated. Figure 21 to 23 shows waveform of overvoltage, GPR at WT#1 and energy consumption of arrester at WT#1, also shows the comparison of voltage, GPR and arrester absorbing energy at different turbine and

grid under lightning chopped tail time. The results indicate that the maximum voltage and the GPR located at turbines and grid were increased in case of chopped time near lightning peak value. Also, the absorbed energy by the arresters located at the turbines and grid is increased.

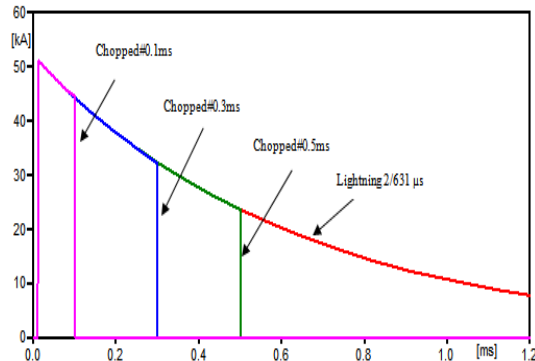


Figure 20. Lightning 2/631 μ s, chopped tail time at 0.1, 0.3, 0.5 ms

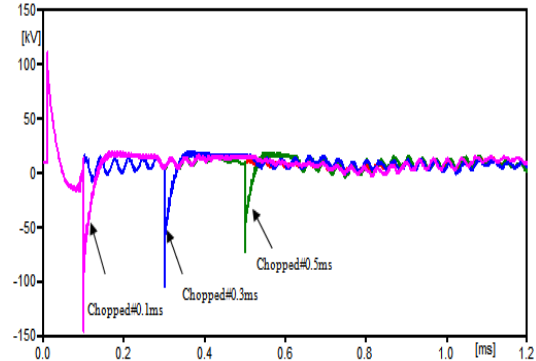


Figure 21. Overvoltages @WT#1 under Lightning 2/631 μ s, chopped tail time at 0.1, 0.3, 0.5 ms

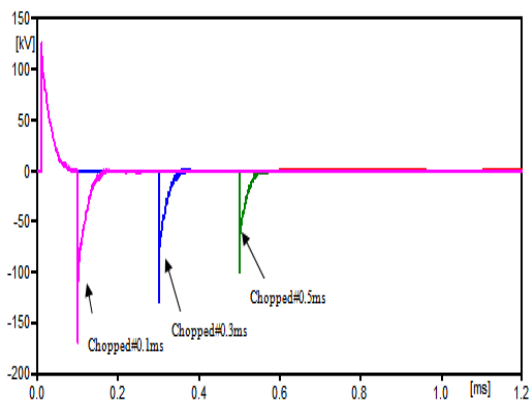


Figure 22. GPR @WT#1 under Lightning 2/631 μ s, chopped tail time at 0.1, 0.3, 0.5 ms

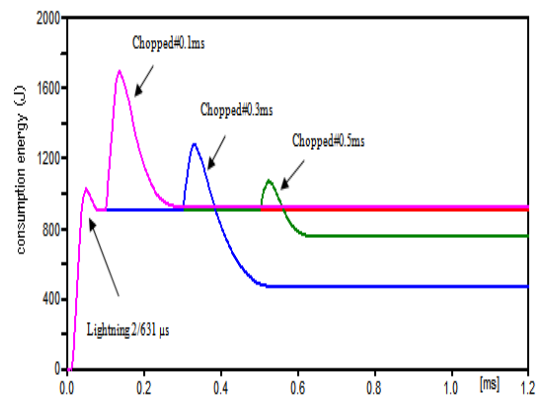


Figure 23. SA consumption energy @WT#1 under Lightning 2/631 μ s, chopped tail time at 0.1, 0.3, 0.5 ms

5. Conclusion

In this paper lightning surge analyses on a wind farm was performed using ATP/EMTP. Lightning hits WTs creates an overvoltage at both HV and LV sides of the boost transformers. The very high surge voltage would appear at struck turbine. Several factors may contribute to a transformer failure and surge arrester burnout due to lightning overvoltage including, crest lightning current, rise time, tail time, lightning inception angle, multiple lightning strike, chopped lightning current and position of lightning. From the results of several analyses the following conclusions were drawn, the result shows that impulse current crest, small front time and large tail time may be the most serious. Also the absorbed energy of surge arresters at negative peak inception instant is within limits but higher than those at zero crossing and positive peak instants. Lightning hit current carrying conductor is more severe than lightning hit noncurrent carrying conductor as tower and nacelle. Multiple strikes don't affect on peak value of overvoltage and GPR, but has a great effect on energy consumption of SA. The maximum voltage and the GPR located at turbines and grid are increased in case of current chopped at tail wave at time near lightning peak value. So this paper provides a practical procedure of lightning protection i.e. lightning current-time characteristic and position of lightning and

chopped lightning current are the main parameters to select an appropriate protection measure for the WT.

References

- [1] IEC TR 61400-24. Wind Turbine Generator Systems-Part 24: Lightning Protection. 2002.
- [2] Yasuda Y, Funabashi T. Analysis on Back-Flow Surge in Wind Farms. IPST'07, Lyon, France. 2007.
- [3] JC Das. Transients in Electrical Systems, Analysis, Recognition and mitigation. 2nd Edition, John Wiley and Sons, Inc. 2010.
- [4] Jheng-Lun Jiang, Hong-Chan Chang, Cheng-Chien Kuo. Analysis of transient energy affection for wind farm under lightning. *Energy*. 2012; 48: 292e297. www.elsevier.com/locate/energy
- [5] Jheng-Lun Jiang, Hong-Chan Chang, Cheng-Chien Kuo, Cheng-Kai Huang. Transient overvoltage phenomena on the control system of wind turbines due to lightning strike. *Renewable Energy*. 2013; 57: 181-189
- [6] Amr M Abd Elhady, Nehmdoh A Sabiha, Mohamed A Izzularab. *Overvoltage Investigation Of Wind Farm Under Lightning Strokes*. IET Conference on Renewable Power Generation (RPG). 2011.
- [7] T Hara, O Yamamoto. Modeling of a Transmission Tower for Lightning-surge Analysis. *IEE Generation, Transmission and Distribution*. 1996; 143(3): 283-289.
- [8] J Marti. Accurate Modeling of Frequency Dependent Transmission Lines in Electromagnetic Transients Simulation. *IEEE Transactions on Power Apparatus and Systems*. 1982; PAS-101(1): 147–157.
- [9] IEEE working Group 3.4.11, Application of Surge Protective Devices Subcommittee Surge Protective Devices Committee. Modeling of Metal Oxide Surge Arresters. *IEEE Transactions on Power Delivery*. 1992; 7(1): 302-309.
- [10] P Pinceti, M Giannetoni. A Simplified Model for Zinc Oxide Surge Arresters. *IEEE Transactions on Power Delivery*. 1999; 14(2): 393-398.
- [11] Nehmdoh A Sabiha, Matti Lehtonen. Lightning-Induced Overvoltages Transmitted Over Distribution Transformer With MV Spark-Gap Operation Part II: Mitigation Using LV Surge Arrester. *IEEE Transactions On Power Delivery*. 2010; 25(4).
- [12] Amr M Abd-Elhady, Nehmdoh A Sabiha, Mohamed A Izzularab. Evaluation of Different Grounding Models for Studying Backflow Current-Overvoltages in Wind Farm. International Middle East Power Systems Conference (MEPCON'12). Cairo, Egypt. 2012.
- [13] ANSI/IEEE Std 80-1986" AC SUBSTATION GROUNDING"
- [14] Yoh Yasuda. Wind Energy Conversion Systems. *Green Energy and Technology* 2012: 243-265.
- [15] Yasuda Y, Kobayashi H, Funabashi T. Surge analysis on wind farm when winter lightning strikes. *IEEE Trans Energy Conversion*. 2008; 23(1): 257-6.
- [16] Schmitt H, Winter W. Simulation of lightning overvoltages in electrical power systems. IPST '01. Brazil: 2001.
- [17] Thuan Q Nguyen, Thinh Pham, Top V Tran. *Electromagnetic Transient Simulation of lightning overvptages in a Wind Farm*. Electrical Insulation Conference, Ottawa, Ontario, Canada. 2013.
- [18] Michael A Omidiora, Matti Lehtonen. *Simulation of Combined Shield Wire and MOV Protection on Distribution Lines in Severe Lightning Areas*. Proceedings of the World Congress on Engineering and Computer Science WCECS, San Francisco, USA. 2007.